

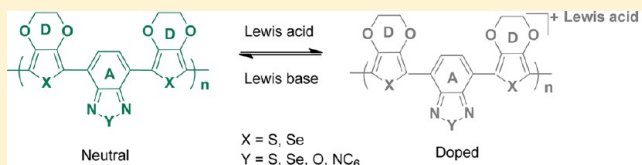
# Unusual Doping of Donor–Acceptor-Type Conjugated Polymers Using Lewis Acids

Elena Poverenov,<sup>\*,‡</sup> Natalia Zamoshchik, Asit Patra,<sup>†</sup> Yonatan Ridelman, and Michael Bendikov

Department of Organic Chemistry, Weizmann Institute of Science, Rehovot, 76100, Israel

**S** Supporting Information

**ABSTRACT:** Conjugated polymers that can undergo unusual nonoxidative doping were designed. A series of polymers based on donor–acceptor–donor (DAD) moieties 2,1,3-benzosele-nadiazole, 2,1,3-benzothiadiazole, 2,1,3-benzoxadiazolebenzo-[2,1,5]oxadiazole, and 2-hexylbenzotriazole as acceptor fragments and 3,4-ethylenedioxythiophene (EDOT) and 3,4-ethylenedioxythiophene (EDOT) as donor fragments were prepared. When the studied polymers were reacted with Lewis acids and bases, notable optical switching and conductivity changes were observed, evidencing the exceptional case of efficient nonoxidative doping/dedoping. Remarkably, in previously reported works, coordination of Lewis acids causes band gap shift but not doping of the conductive polymer, while in the present study, coordination of Lewis acid to highly donating EDOT and EDOS moieties led to polymer doping. The polymers show remarkable stability after numerous switching cycles from neutral to doped states and vice versa and can be switched both electrochemically and chemically. The reactivity of the prepared polymers with Lewis acids and bases of different strengths was studied. Calculation studies of the Lewis acid coordination mode, its effect on polymer energies and band gap, support the unusual doping. The reported doping approach opens up the possibility to control the conjugation, color change, and switching of states of conjugated polymers without oxidation.



## INTRODUCTION

The doping and dedoping of conjugated polymers is a basic process that provides them with attractive electronic and optical properties.<sup>1,2</sup> Doping leads to a significant decrease in the polymer band gap that causes conductivity and color changes in the material. Because of their dopability and other outstanding properties, organic conjugated polymers represent a very important class of materials from both fundamental and practical perspectives.<sup>1,3–7</sup> Usually, doping of organic polymers is achieved by oxidation/reduction (through the supply or removal of electrons), which can be done chemically or electrochemically. Oxidative doping, both chemical and electrochemical, is a well-studied and documented approach that has been widely adopted.<sup>1,2,8</sup> By contrast, nonoxidative doping is highly unusual. It is mostly known only for polyanilines,<sup>9</sup> where doping is generally performed using protonation by Bronsted acids and rarely using Lewis acids.<sup>10</sup> For other organic conjugated polymers nonoxidative doping is scantily studied,<sup>11</sup> and if an acidic reagent was present, it was usually utilized only as a catalyst to achieve a better polymerization process.<sup>12</sup>

Low band gap conducting polymers are of particular interest for their electrochemical and optical properties and offer a wide spectrum of advanced properties that can be tuned to meet various applicative demands.<sup>13,14</sup> They are promising candidates as a light absorbing component in organic solar cells<sup>15,16</sup> and for electrochromic materials.<sup>1,2,17</sup> One of the most successful approaches to low band gap polymers is to design an alternating sequence of donor–acceptor–donor (DAD) units<sup>18</sup> in the  $\pi$ -conjugated chain, where the interaction

between alternating donor and acceptor units increases the double bond character of the polymer backbone and leads to significant compression of the band gap.<sup>19</sup> Various combinations of donors and acceptors have been used to optimize polymer properties, for instance, thiophene and (3,4-ethylenedioxythiophene) (EDOT)-based donor–acceptor  $\pi$ -conjugated low band gap polymers.<sup>20</sup> Several of these conjugated copolymers contain 2,1,3-benzothiadiazole as the electron-acceptor unit.<sup>21</sup>

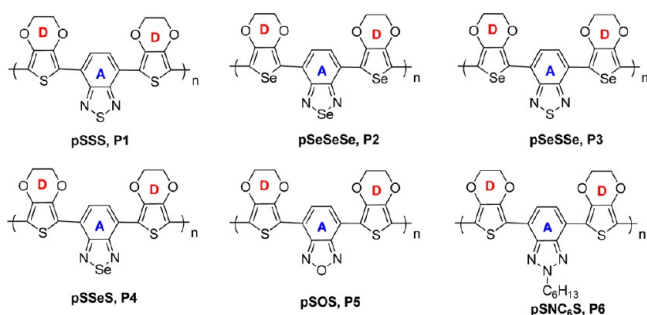
The influence of Lewis acid coordination on donor–acceptor polymers was noticed by Bazan group. In 2009 Bazan reported a narrowing of a band gap of the conjugated oligomers upon coordination of Lewis acid to nitrogen of benzothiadiazole fragment.<sup>22</sup> Interestingly, when benzothiadiazole was replaced by pyridalithiadiazole coordination of Lewis acid,  $B(C_6F_5)_3$  was redirected to a more basic pyridine (and not thiadiazole) nitrogen site that led to stronger B–N interactions and formation of NIR-absorbing polymers.<sup>23</sup> Recently, Bazan and Nguyen groups also reported color tuning and mobility enhancement of conductive polymers by formation of adducts with Lewis acids.<sup>24</sup>

In the present work, a series of DAD polymers **P1–P6** that contain highly donating EDOT or EDOS moieties was studied. Polymers **P1**<sup>25</sup> and **P4**<sup>26</sup> were previously reported, and polymers **P2**, **P3**, **P5**, and **P6** are prepared in this study for the first time. We have found that reaction with Lewis acid

Received: January 29, 2014

Published: March 7, 2014

causes not only band gap shift, but also doping of the prepared polymers. The conductivity changes and large optical switching revealed an effective doping process that took place without electron transfer. As a consequence of the doping process, reaction of the doped polymers with Lewis base led to their "neutralization" and thus dedoping. The polymers showed good stability even after multiple switching cycles. For comparison, an electrochemical doping/dedoping was also performed. The reported nonoxidative doping approach is reversible, nondestructive, and can be regulated by the amount of added Lewis acid or base. This is a simple chemical postsynthetic method that allows for the control of conjugation, color, and conductivity of the conjugated polymers.



## EXPERIMENTAL METHODS

**Synthesis and Characterization.**  $^1\text{H}$  NMR and  $^{13}\text{C}$  NMR spectra were recorded on a 300 MHz spectrometer as a solution in  $\text{CDCl}_3$  with tetramethylsilane (TMS) as the external standard. Columns were prepared with silica gel (60–230 mesh). High resolution mass spectra were measured on a Waters Micromass GCT Premier Mass Spectrometer using field desorption (FD) ionization.

2-(Tributylstannyl)-3,4-ethylenedioxythiophene (**8a**),<sup>27</sup> dihydrothieno[3,4-*b*]-1,4-dioxin-5-yl)benzo[2,1,5]thiadiazole (**1**),<sup>25</sup> and 4,7-bis(2,3-dihydrothieno[3,4-*b*]-1,4-dioxin-5-yl)benzo[2,1,5]selenadiazole (**4**)<sup>26</sup> were synthesized according to the reported procedures.

2-(Tributylstannyl)-3,4-ethylenedioxythiophene (**8b**). To a stirred solution of 3,4-ethylenedioxythiophene (EDOS, **7b**; 230 mg, 1.2 mmol) in tetrahydrofuran (THF, 8 mL) at  $-78^\circ\text{C}$  (acetone/dry ice bath) under an inert atmosphere, a solution of *n*BuLi (1.6 M, 0.8 mL, 1.28 mmol in hexane) was added dropwise. The resulting solution was brought to room temperature and stirred for 1 h. The reaction mixture was again cooled to  $-78^\circ\text{C}$ , and tributyltin chloride (420 mg, 0.35 mL, 1.30 mmol) was added. Then the reaction mixture was brought to room temperature and stirred for 6 h. The red colored reaction mixture was then quenched with 10%  $\text{NH}_4\text{Cl}$  (15 mL), and the resulting solution was diluted with  $\text{H}_2\text{O}$  (50 mL). The aqueous layers were extracted with ether (40 mL). The combined extracts were washed with brine, water, dried ( $\text{MgSO}_4$ ), and concentrated. The crude residue was purified by column chromatography on silica (washed with  $\text{Et}_3\text{N}$ ) to furnish compound 2-(tributylstannyl)-3,4-ethylenedioxythiophene, **8b** (500 mg, 86%) as a light green oil:  $^1\text{H}$  NMR (250 MHz,  $\text{CDCl}_3$ )  $\delta$  7.02 (s, 1H), 4.11 (s, 4H), 1.59–1.47 (m, 6H), 1.35–1.26 (m, 6H), 1.10–1.03 (m, 6H), 0.89 (t,  $J = 7.25$  Hz, 9H);  $^{13}\text{C}$  NMR (100 MHz,  $\text{CDCl}_3$ )  $\delta$  143.4, 127.9, 107.2, 101.6, 64.2, 64.2, 28.9, 27.1, 13.6, 10.7; HRMS for  $\text{C}_{18}\text{H}_{32}\text{O}_2\text{SeSn}$  [ $\text{M}^+$ ] calcd 478.1000, found 478.0607.

4,7-Bis(2,3-dihydro-seleno[3,4-*b*]-1,4-dioxin-5-yl)benzo[2,1,5]-selenadiazole (**2**). To a stirred solution of 2-(tributylstannyl)-3,4-ethylenedioxythiophene (**8b**; 200 mg, 0.42 mmol) in dry toluene (10 mL) at room temperature were successively added 4,7-dibromo-2,1,3-benzoselenodiazole<sup>28</sup> (**9b**; 70 mg, 0.21 mmol) and  $(\text{Ph}_3\text{P})_4\text{Pd}$  (25 mg, 0.02 mmol) under a nitrogen atmosphere. The resulting solution was heated at reflux for overnight. After completion of the

reaction, the mixture was diluted with  $\text{CH}_2\text{Cl}_2$  (200 mL). The organic layer was successively washed with water (30 mL), brine (30 mL), water (30 mL), dried ( $\text{MgSO}_4$ ), and concentrated. The crude product was purified by column chromatography on silica gave compound **2** (75 mg, 66%) as a deep red solid:  $^1\text{H}$  NMR (250 MHz,  $\text{CDCl}_3$ )  $\delta$  8.53 (s, 2H), 7.02 (s, 2H), 4.42–4.36 (m, 4H), 4.31–4.25 (m, 4H);  $^{13}\text{C}$  NMR (100 MHz,  $\text{CDCl}_3$ )  $\delta$  152.5, 142.8, 141.4, 126.2, 124.9, 115.6, 105.2, 64.7, 64.0; UV-vis ( $\text{CH}_2\text{Cl}_2$ )  $\lambda_{\text{max}} = 505$  nm.

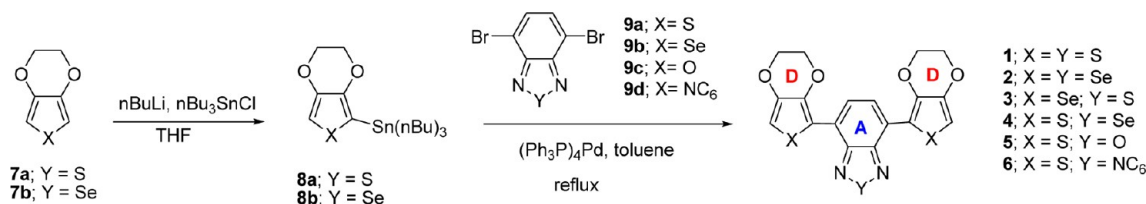
4,7-Bis(2,3-dihydro-seleno[3,4-*b*]-1,4-dioxin-5-yl)benzo[2,1,5]-thiadiazole (**3**). To a stirred solution of 2-(tributylstannyl)-3,4-ethylenedioxythiophene (**8b**; 400 mg, 0.84 mmol) in dry toluene (20 mL) at room temperature were successively added 4,7-dibromo-2,1,3-benzothiadiazole (**9a**; 120 mg, 0.41 mmol) and  $(\text{Ph}_3\text{P})_4\text{Pd}$  (45 mg, 0.04 mmol) under a nitrogen atmosphere. The resulting solution was heated at reflux for 15 h. After completion of the reaction, the mixture was diluted with  $\text{CH}_2\text{Cl}_2$  (250 mL). The organic layer was successively washed with water (40 mL), brine (30 mL), water (35 mL), dried ( $\text{MgSO}_4$ ), and concentrated. The crude product was purified by column chromatography on silica gel (50% dichloromethane–hexane) to give compound **3** (130 mg, 63%) as a deep red solid:  $^1\text{H}$  NMR (400 MHz,  $\text{CDCl}_3$ )  $\delta$  8.53 (s, 2H), 7.02 (s, 2H), 4.41–4.37 (m, 4H), 4.30–4.25 (m, 4H);  $^{13}\text{C}$  NMR (100 MHz,  $\text{CDCl}_3$ )  $\delta$  152.5, 142.8, 141.4, 126.2, 124.9, 115.6, 105.2, 64.7, 64.0; HRMS for  $\text{C}_{18}\text{H}_{12}\text{N}_2\text{O}_4\text{S}_2\text{Se}_2$  [ $\text{M}^+$ ] calcd 511.8848, found 511.8846; UV-vis ( $\text{CH}_2\text{Cl}_2$ )  $\lambda_{\text{max}} = 503$  nm.

4,7-Bis(2,3-dihydro-thieno[3,4-*b*]-1,4-dioxin-5-yl)benzo[2,1,5]-oxadiazole (**5**). To a stirred solution of 2-(tributylstannyl)-3,4-ethylenedioxythiophene (**8a**; 750 mg, 1.74 mmol) in dry toluene (25 mL) at room temperature were successively added 4,7-dibromo-2,1,3-benzoxadiazole<sup>29</sup> (**9c**; 240 mg, 0.86 mmol) and  $(\text{Ph}_3\text{P})_4\text{Pd}$  (90 mg, 0.08 mmol) under a nitrogen atmosphere. The resulting solution was heated at reflux for overnight. After completion of the reaction, the mixture was diluted with  $\text{CH}_2\text{Cl}_2$  (200 mL). The organic layer was successively washed with water, brine, dried ( $\text{MgSO}_4$ ), and concentrated. The crude product was purified by column chromatography on silica gel (dichloromethane–hexane) to give compound **5** (220 mg, 63%) as a red solid:  $^1\text{H}$  NMR (400 MHz,  $\text{CDCl}_3$ )  $\delta$  8.11 (s, 2H), 6.56 (s, 2H), 4.45–4.39 (m, 4H), 4.31–4.25 (m, 4H);  $^{13}\text{C}$  NMR (125 Mz,  $\text{CDCl}_3$ )  $\delta$  147.7, 141.8, 140.6, 127.5, 119.3, 112.6, 102.5, 65.0, 64.3; HRMS for  $\text{C}_{18}\text{H}_{12}\text{N}_2\text{O}_5\text{S}_2$  [ $\text{M}^+$ ] calcd 400.0188, found 400.0185; UV-vis ( $\text{CH}_2\text{Cl}_2$ )  $\lambda_{\text{max}} = 475$  nm.

4,7-Bis(2,3-dihydro-thieno[3,4-*b*]-1,4-dioxin-5-yl)benzo[2,1,5]-hexylbenzotriazole (**6**). To a well stirred solution of 2-(tributylstannyl)-3,4-ethylenedioxythiophene (**8a**; 860 mg, 2.00 mmol) and 4,7-dibromo-2-hexylbenzohexyltriazole<sup>30</sup> (**9d**; 361 mg, 1.00 mmol) in toluene (20 mL) at room temperature was added  $(\text{Ph}_3\text{P})_4\text{Pd}$  (100 mg, 0.09 mmol) under a nitrogen atmosphere, and the resulting mixture was heated at reflux for 20 h. After completion of the reaction, the mixture was diluted with  $\text{CH}_2\text{Cl}_2$  (150 mL). The organic layer was successively washed with water (50 mL), brine (30 mL), water (40 mL), dried ( $\text{MgSO}_4$ ), and concentrated. The crude product was purified by column chromatography on silica gel (dichloromethane–hexane) to give compound **6** (300 mg, 62%) as a yellow solid:  $^1\text{H}$  NMR (400 MHz,  $\text{CDCl}_3$ )  $\delta$  8.09 (s, 2H), 6.46 (s, 2H), 4.77 (t,  $J_{\text{H-H}} = 7$  Hz, 2H), 4.38–4.26 (m, 8H), 3.67 (q,  $J_{\text{H-H}} = 7$  Hz, 2H), 2.14 (m, 2H), 1.31–1.24 (m, 4H), 0.86 (t,  $J_{\text{H-H}} = 7$  Hz, 3H);  $^{13}\text{C}$  NMR (125 Mz,  $\text{CDCl}_3$ )  $\delta$  147.7, 141.7, 139.44, 123.63, 121.21, 114.08, 100.60, 64.91, 64.44, 56.73, 31.24, 29.97, 22.49, 18.43, 14.01; HRMS for  $\text{C}_{24}\text{H}_{25}\text{N}_3\text{O}_4\text{S}_2$  [ $\text{M}^+$ ] calcd 483.1286, found 483.1287; UV-vis ( $\text{CH}_2\text{Cl}_2$ )  $\lambda_{\text{max}} = 400$  nm.

**Electro- and Spectroelectrochemistry.** All chemicals were purchased from the Sigma-Aldrich chemical company. Electrochemical studies were carried out with a Princeton Applied Research 263A potentiostat using Pt electrode and an indium tin oxide (ITO) coated glass slide as the working electrode ( $7 \times 50 \times 0.7$  mm,  $R_s = 8$ –12  $\Omega$ , Delta Technologies Inc.), a platinum wire as the counter electrode, and an AgCl coated Ag wire, which was directly dipped into the electrolyte solution,<sup>31</sup> as the reference pseudo-electrode. All potentials were calibrated using the  $\text{Fc}/\text{Fc}^+$  standard, which is 0.34 V under these conditions,<sup>32</sup> and reported potentials were recalculated to the

Scheme 1. Synthesis of Monomers 1–6



saturated calomel electrode (SCE) scale. The experimental values of the HOMO energy levels were obtained from the onset of the oxidation peak in CV scans of each polymer film in monomer free solution. To relate the measured potentials to the vacuum level, we used the following equation: HOMO (eV) =  $E_{\text{onset}} + 4.4$ , where 4.4 eV is the SCE energy level relative to the vacuum.<sup>33,34</sup> Experimental values for the LUMO levels were obtained using  $E(\text{LUMO}) = E(\text{HOMO}) + E_{\text{g}(\text{exp})}$ , where  $E_{\text{g}(\text{exp})}$  is the band gap obtained from the onset of the absorption peak of the neutral polymer.

The polymer films were prepared by electropolymerization of the corresponding monomer on ITO-coated glass slides (working area of  $0.7 \times 3.2 \text{ cm}^2$ ) using tetra-*n*-butylammonium hexafluorophosphate (TBAPF<sub>6</sub>) as a supporting electrolyte and methylene chloride as a solvent. The solution was purged with nitrogen before polymerization to remove any incipient oxygen. The films were prepared using the cyclic voltammetry (CV) mode. Before examining the optical properties of the polymers, the films were rinsed with acetonitrile.

UV–vis–NIR spectra were recorded on a V-570 JASCO UV–vis–NIR spectrophotometer. In spectroelectrochemical measurements, the working electrode was an ITO-coated glass slide, the counter electrode was a platinum wire, and Ag/AgCl was used as the reference pseudo-electrode. The spectroelectrochemical measurements were performed in methylene chloride using TBAPF<sub>6</sub> as a supporting electrolyte.

**Doping and Dedoping.** Chemical doping/dedoping was performed in the following way: the ITO slide with polymer film was immersed into a solution of the doping/dedoping reagent under nitrogen for 30–60s and then thoroughly rinsed 2–3 times with acetonitrile, and its UV–vis–NIR spectrum was measured. Methylene chloride solutions of boron trifluoride diethyl etherate, BF<sub>3</sub>O(C<sub>2</sub>H<sub>5</sub>)<sub>2</sub> or shortly BF<sub>3</sub> (0.04 M), triphenyl borate, BPhe<sub>3</sub> (0.04 M), and trimethyl borate, BMe<sub>3</sub> (0.04 M) were utilized for doping experiments, while dedoping was performed in an acetonitrile solution containing potassium bis(trimethylsilyl)amide (0.05 M) and Et<sub>3</sub>N (0.1 M). All the presented polymer P1–P6 films underwent the following process: (a) electrochemical dedoping to obtain the neutral polymer; (b) treatment with a weak Lewis acid (BMe<sub>3</sub>) to study how easily the specific polymer undergoes chemical doping; (c) treatment with a stronger Lewis acid (BPhe<sub>3</sub>) to examine the importance of acid strength to chemical doping; (d) treatment with a strong Lewis acid (BF<sub>3</sub>) to determine the maximal doping level achieved by an external reagent; (e) treatment with a moderate base (Et<sub>3</sub>N) to investigate how easily the specific polymer undergoes chemical dedoping; (f) electrochemical doping to obtain a maximally doped polymer.

**Conductivity.** Conductivity measurements have been performed on polymers that were polymerized on interdigitated electrode (ABTECH Scientific, Inc.) utilizing polymerization conditions reported for each polymer. The interdigitated electrode is consisting of two arrays of 50 gold digits (strips), each 10 μm wide and 5 mm long with an interdigit distance of 10 μm, where only the microarrays were accessible to the electrolyte solution.

The conductivity (resistivity) of the prepared polymers was measured by multimeter. The conductivity of electrochemically doped and dedoped polymers was measured first. Then neutral (dedoped) polymers were immersed in solution of BF<sub>3</sub> (0.4 M) in methylene chloride, and their conductivity (resistivity) was measured. Conductivity (resistivity) of the air doped polymers was also measured by exposing neutral polymers to air for 1 h.

**Calculations.** Computational studies were carried out using density functional theory (DFT) with the Gaussian 09 series of programs.<sup>35</sup> The geometries of the polymers were fully optimized using the periodic boundary conditions (PBC) formalism and hybrid DFT with Becke's three-parameter exchange functional combined with the LYP correlation functional (B3LYP) and the 6-31G(d) basis set.<sup>36</sup> Highest occupied crystal orbital (HOCO) and lowest unoccupied crystal orbital (LUCO) were calculated to study a doping effect on polymers energy gap.

## RESULTS AND DISCUSSION

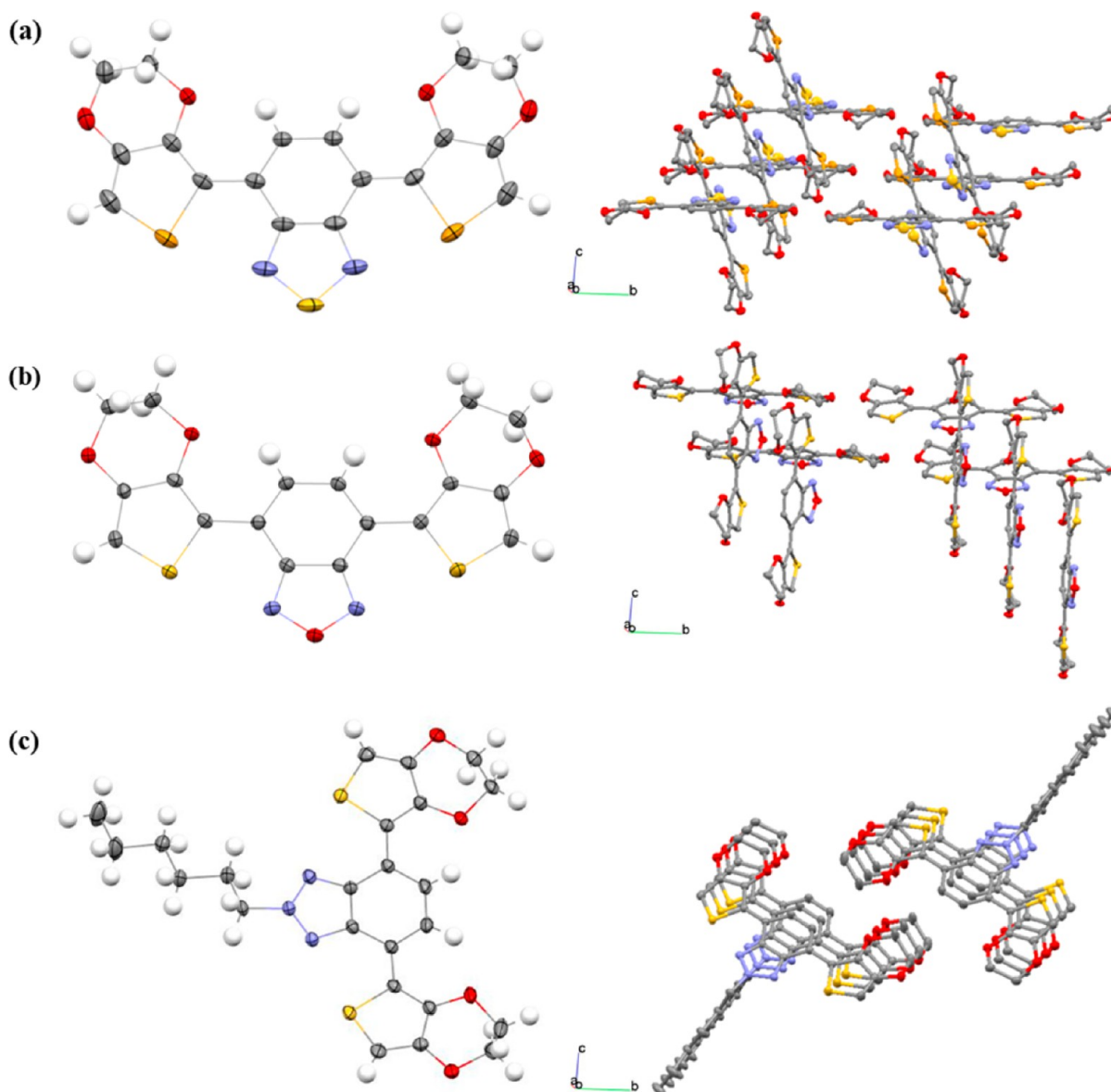
**Synthesis of Monomers 1–6 and X-ray Studies.** 2-Tributylstannyl-3,4-ethylenedioxythiophene (8a) was synthe-

Table 1. Electrochemical and Spectroelectrochemical Properties of the DAD Polymers, P1–P6

	$E_{\text{ox,mon,onset}}^a$ (V vs SCE)	$E_{\text{ox,pol,onset}}^b$ (V vs SCE)	$\lambda_{\text{max,mon}}^c$ (nm)	$\lambda_{\text{max,pol}}^d$ (nm)	$E_{\text{g,exp}}^e$ (eV)
pSSS, P1	0.78	−0.47	480	775	1.19
pSeSeSe, P2	0.73	−0.51	503	843	1.10
pSeSSe, P3	0.63	−0.59	503	819	1.13
pSSeS, P4	0.75	−0.43	518	830	1.21
pSOS, P5	0.85	−0.37	474	767	1.26
pSNC <sub>6</sub> S, P6	0.64	−0.30	400	624/684	1.65

<sup>a</sup>The onset of the oxidation potential calculated from the CV of a monomer. <sup>b</sup>The onset of the oxidation potential calculated from the CV of polymer film in a monomer-free electrolyte solution. <sup>c</sup>Absorption maxima of the monomers. <sup>d</sup>Absorption maxima of the polymers in the neutral (undoped) states. <sup>e</sup>The experimental optical band gap obtained from the onset of the longest UV–vis absorption peak.

sized from EDOT (7a) according to the reported procedure.<sup>31</sup> 2-Tributylstannyl-3,4-ethylenedioxysephenone (8b) was obtained from EDOS<sup>37</sup> (7b), by reacting with *n*BuLi and tributylstannyl chloride in THF, in 86% yield as an oil (Scheme 1). Compound 8b was subjected to Stille coupling with 4,7-dibromo-2,1,3-benzoselenadiazole (9b) to provide monomer 2 as a dark red solid with a 66% yield. Similarly, Stille coupling of 8b with 4,7-dibromo-2,1,3-benzothiadiazole (9a) in the presence of (Ph<sub>3</sub>P)<sub>4</sub>Pd in refluxing toluene gave monomer 3 with a 63% yield as a dark red solid. Monomer 5 was prepared as a red solid in 63% yield from coupling between 8a and 4,7-dibromo-2,1,3-benzoxadiazole (9c), while monomer 6 was prepared as a yellow solid in 62% yield from 8a and 4,7-dibromo-2-hexylbenzotriazole (9d). The monomers 1<sup>25</sup> and 4<sup>26</sup> were synthesized according to reported procedures from 8a reacting with 9a and 9b, respectively. The absorption spectrum of the prepared DAD monomers significantly depends on a heteroatom in the acceptor unit. The monomers 2 and 4 (selenium in acceptor unit) have maximum absorbance at 503 and 518 nm, respectively, the monomers 1 and 3 (sulfur in



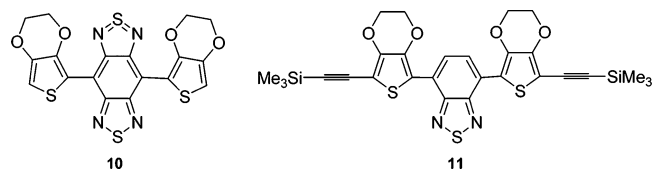
**Figure 1.** X-ray crystal structures of compounds 3 (a), 5 (b), and 6 (c). Left is single molecules and right is packing structures.

acceptor unit) have maximum absorbance at 480 and 503 nm, respectively, the monomer 5 (oxygen in acceptor unit) has maximum absorbance at 474 nm. A significant shift in UV-vis spectra is obtained for monomer 6 that has  $\text{NC}_6\text{H}_{13}$  group in acceptor unit; this monomer has maximum absorbance at 400 nm. (Table 1 and Figure S1, Supporting Information).

X-ray structures of monomers 3, 5, and 6 were obtained by recrystallization of these compounds from the mixture of  $\text{CH}_2\text{Cl}_2$  and hexane at room temperature (Figure 1).

DAD structures 3 and 5 (Figure 1a,b) have packing mode of different groups of nearly parallel molecules. The molecules inside each group are shifted in relative to each other; therefore, their aromatic rings are not situated on the same axes, and that in turn decreases, or even avoids,  $\pi$ - $\pi$  stacking. The packing order and  $\pi$ - $\pi$  stacking can be dictated by side chain as in case of monomer 6 (Figure 1c) that demonstrates structured arrangement of the molecules in parallel manner. This observation is in line with the previously reported structures of this type.<sup>38,39</sup> For instance, in the reported X-ray structure of DAD 1 no evidence of any packing ordering is obtained.<sup>38</sup> The

same phenomenon is observed for additional thiadiazole ring substituted 10.<sup>39</sup> On the other hand, trimethylsilyl acetylene side chain substituted comonomer 11 shows a parallel arrangement similar to that of our monomer 6.<sup>38</sup>



**Electrochemical Polymerization and Optical Characterization.** The electropolymerizations of the monomers 1–6 resulted in polymer films P1–P6 that revealed both p- and n-doping and a stable reversible redox process after repeated cycles in monomer free solvent (Figure 2 and Figure S2, Supporting Information). Electrochemical polymerization and characterization of polymers P1<sup>25</sup> and P4<sup>26</sup> was equivalent to the previously reported. These polymer films P1–P5 are green in the neutral state and change to transparent light blue in the

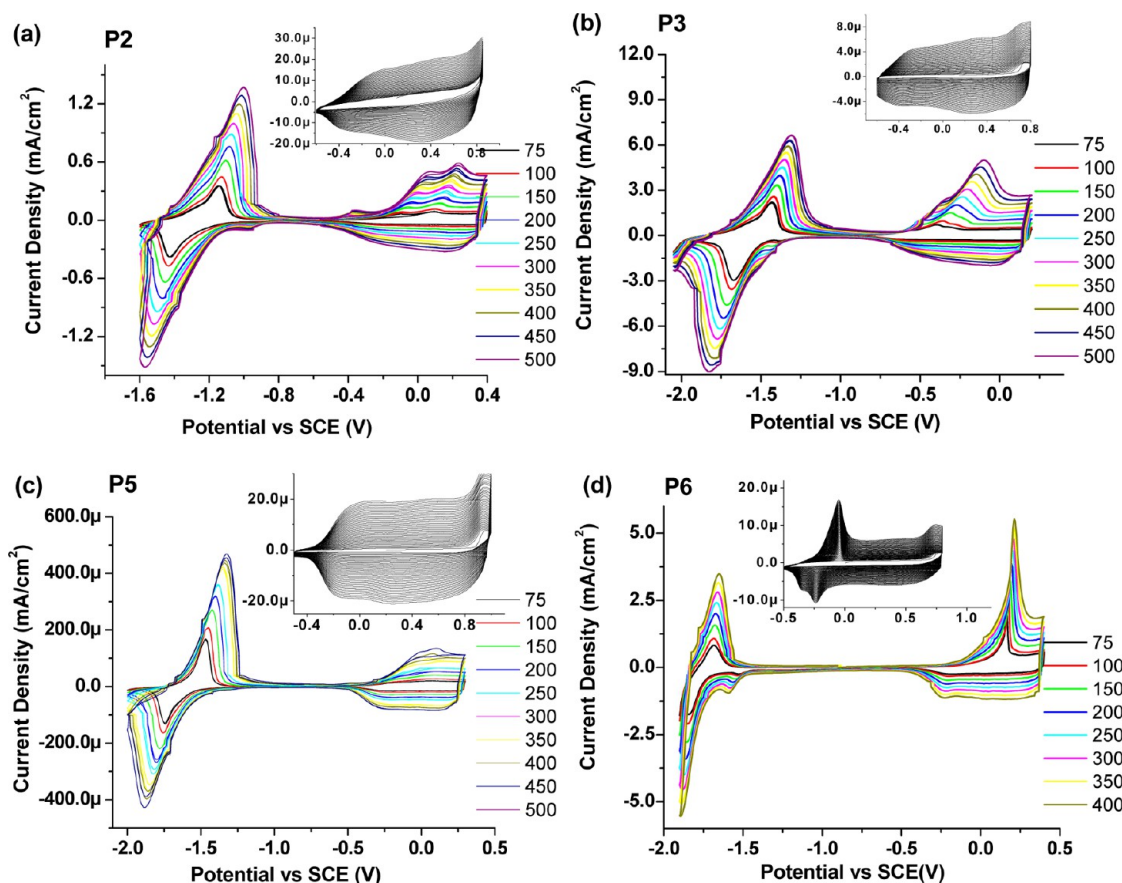


**Figure 2.** The CV spectra of P2, P3, P5, P6 polymers carried out in monomer free solution using 0.1 M TBAPF<sub>6</sub>/CH<sub>2</sub>Cl<sub>2</sub> and applying different scan rates in mV/s. Inset: the electropolymerizations of monomers 2–6 carried out using 0.1 M TBAPF<sub>6</sub>/CH<sub>2</sub>Cl<sub>2</sub>. (a) pSeSeSe, P2; (b) pSeSSe, P3; (c) pSOS, P5; (d) pSNC<sub>6</sub>S, P6. For pSSeS, P4, see Figure S4, Supporting Information.<sup>40</sup>

oxidized state, while P6 is blue in the neutral state and transparent light blue in the oxidized state. The scan rate dependence of anodic peak and cathodic peak of the polymer films P1–P6 were investigated, and a true linear relation was observed between the peak current and the scan rate. The linear change proportional to the scan rate indicated nondiffusional redox process and well-adhered electroactive polymer films (Figure S3, Supporting Information).

Comparison of the absorption spectra of P1–P6 demonstrates considerable differences between the polymers (Figures 3 and 4, Table 1). The spectroelectrochemically measured band gap (assigned as the onset of the  $\pi$ – $\pi^*$  transition) varies according to the nature of donor–acceptor units. Incorporation of a selenium atom to a donor unit caused a notable decrease in band gap (1.10 eV for pSeSeSe, P2 vs 1.19 eV for pSSS, P1) as was previously shown for polyselenophenes.<sup>41</sup> The band gap of pSOS, P5 (1.26 eV) is higher than that of pSSS, P1, probably because of the presence of a hard oxygen atom in the acceptor unit, while pSNC<sub>6</sub>S, P6 has the highest band gap (1.6 eV) in the series. Polymers P1–P5 have nonsplit red-shifted absorption spectra, and their UV–vis–NIR spectra show two well-separated absorption maxima at 417–460 nm and 775–830 nm in the neutral state, which is necessary for obtaining a green polymer. The spectrum of P6 exhibits a blue-shifted shoulder pattern with  $\lambda_{\text{max}}$  at 624 nm. Perhaps, the shoulder pattern of P6 is a result of alkyl chain substituents that provide the polymer with a more ordered structure.<sup>42</sup>

**Nonoxidative Doping–Dedoping upon Coordination–Decoordination of Lewis Acid.** Neutral pSSS, P1 was rinsed with a solution of BF<sub>3</sub> (0.4 M) in methylene chloride. Immediately, a color change from green to light bluish-gray was observed. UV–vis–NIR spectroscopy revealed doping of P1 by the external Lewis acid. Afterward, the converse process of dedoping was examined. For this purpose, doped P1 was rinsed in a freshly prepared solution of acetonitrile with potassium bis(trimethylsilyl)amide, (Me<sub>3</sub>Si)<sub>2</sub>NK. Instantaneous color conversion to green was observed, and absorption spectra confirmed re-establishment of the undoped (neutral) state. The reverse dedoping process that occurs upon treatment of the polymer with base reveals that it is not electron transfer, but a chemical reaction with a Lewis acid causing formation of doped polymer. Thus, we observed the nonoxidative doping/dedoping that allowed for switching of the studied conjugated polymers.

All polymers from the present series were examined in terms of the possibility of nonoxidative doping/dedoping induced by Lewis acid and base (Scheme 2).

Polymers P1–P5 were successfully switched by external chemical reagents, while pSNC<sub>6</sub>S, P6, which has a significantly higher band gap, showed only partial changes. Both color changes and absorption spectra of polymers P1–P5 revealed good doping and dedoping upon treatment with BF<sub>3</sub> and (Me<sub>3</sub>Si)<sub>2</sub>NK, respectively.<sup>43</sup> Reaction with strong base (Me<sub>3</sub>Si)<sub>2</sub>NK led to full dedoping of P1–P5 polymers, equal to the dedoping that is achieved electrochemically. It is

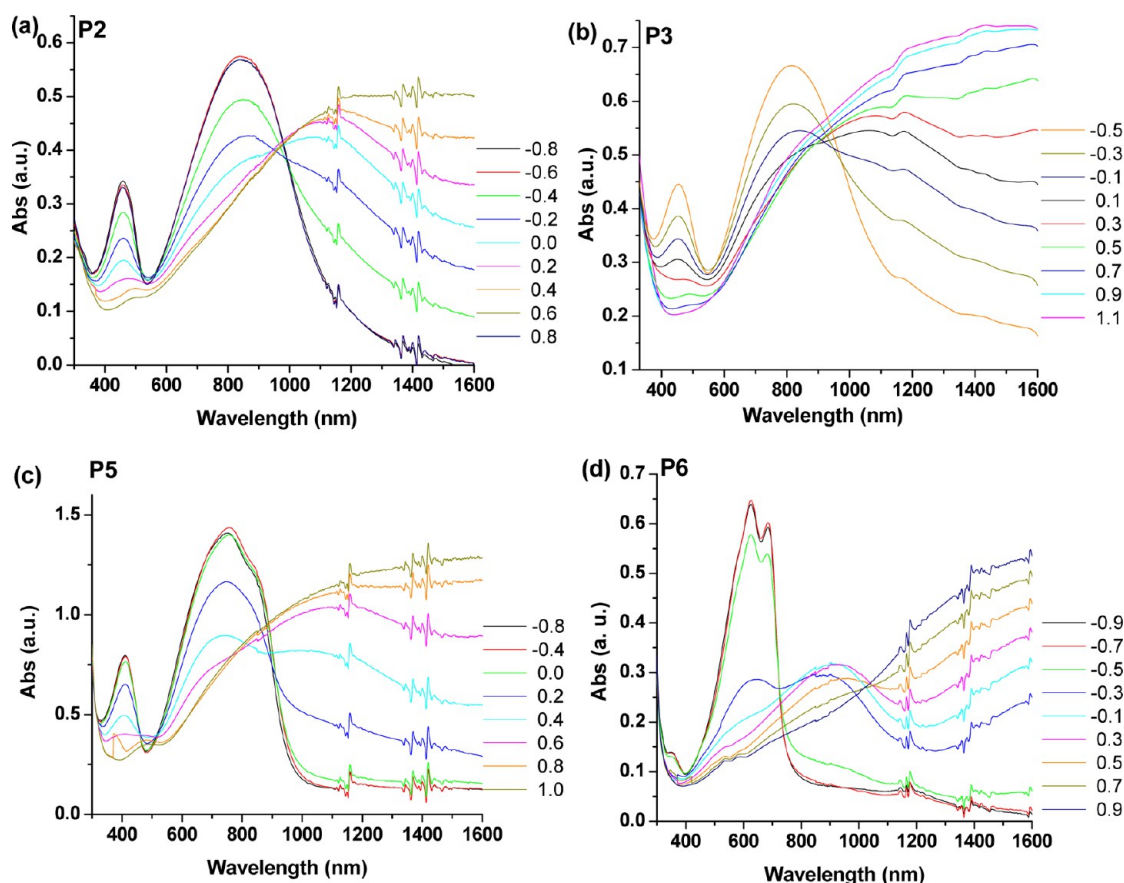


Figure 3. The absorption spectra of DAD polymers P2, P3, P5, and P6 performed in TBAPF<sub>6</sub>/CH<sub>2</sub>Cl<sub>2</sub>.

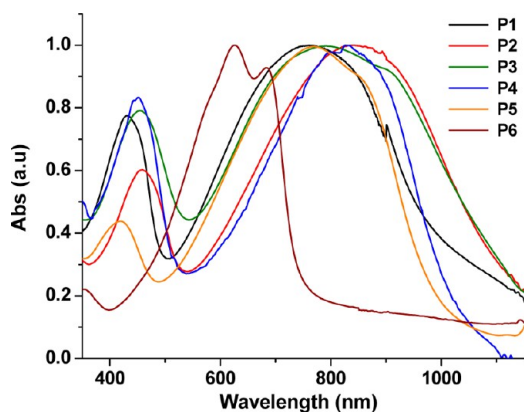


Figure 4. Normalized absorption spectra of DAD polymers P1–P6 in neutral state performed in TBAPF<sub>6</sub>/CH<sub>2</sub>Cl<sub>2</sub>.

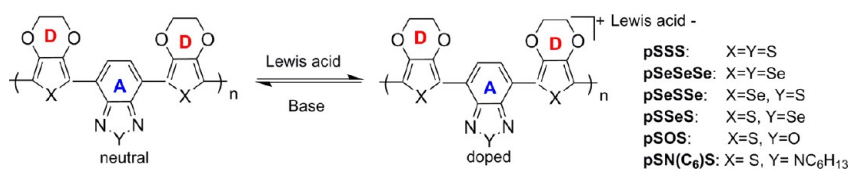
important to note that polymers P1–P5 demonstrate remarkable stability upon switching. No evidence of polymer decomposition was observed after multiplied doping/dedoping cycles. Additionally, we found that doping/dedoping processes

can be combined with electrochemical doping/dedoping processes using any combination of these methods.

The reported results provide a unique example of non-oxidative doping and dedoping of conductive polymers that lay outside the aniline polymers. As was observed by Bazan, coordination of Lewis acid leads to remarkable alternations of polymer properties.<sup>23–25</sup> Bazan observed that coordination of Lewis acids causes significant band gap shift of the conductive polymers. In the present study we found an additional example of the ability of Lewis acid to manipulate properties of conductive polymers: coordination of Lewis acid to highly donating EDOT and EDOS moieties led to polymer doping (see later calculation of energies of frontier orbitals). The nonoxidative doping benefits all advantages of oxidative doping such as polymer band gap decrease, conductivity, and color changes but achieved with no removal of electrons.

**Doping Strength.** To explore the implications of various donor/acceptor fragments, chemical switching of polymers P1–P6 was performed using external reagents of different strengths including Lewis acids BMe<sub>3</sub>, BPh<sub>3</sub>, BF<sub>3</sub> and Lewis base Et<sub>3</sub>N (Figure 5). The relatively weak BMe<sub>3</sub> Lewis acid

#### Scheme 2. Doping/Dedoping Process of Donor–Acceptor-Type Polymers Using an External Lewis Acid and External Base



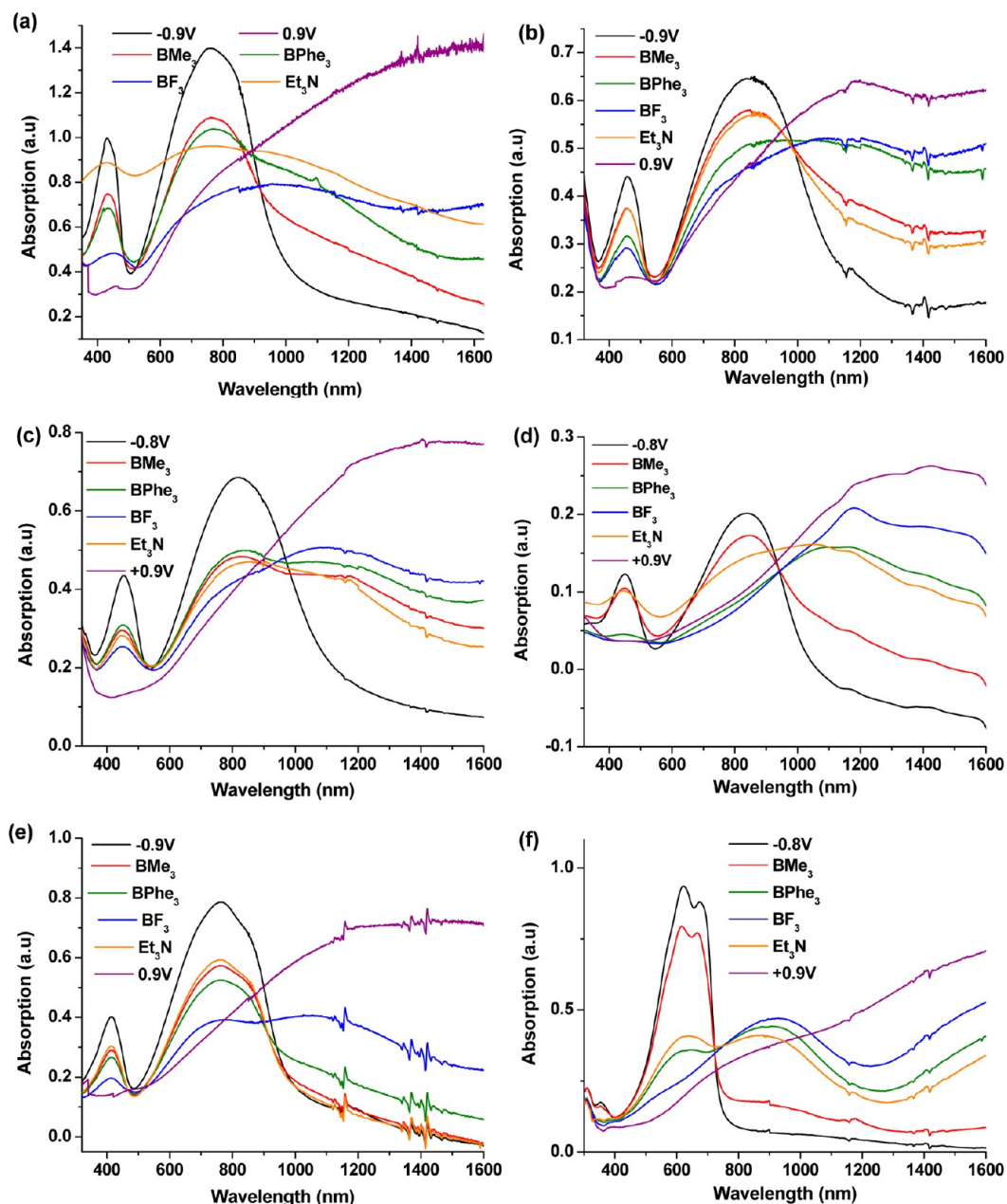


**Figure 5.** Chemical doping and dedoping of DAD polymers with different doping/dedoping reagents and electrochemical doping/dedoping. (a) pSSS, P1; (b) pSeSeSe, P2; (c) pSeSse, P3; (d) pSseS, P4; (e) pSOS, P5; (f) pSNC<sub>6</sub>S, P6. All the presented polymer films underwent the following process: electrochemical dedoping; treatment with BMe<sub>3</sub>; treatment with BPh<sub>3</sub>; treatment with BF<sub>3</sub>; treatment with Et<sub>3</sub>N; electrochemical doping.

**Table 2.** Calculated and Experimental Energy Levels and Band Gap Calculated at the PBC/B3LYP/6-31G(d) Level of Theory of Various Donor–Acceptor (DA) Polymers

	HOCO <sub>calc</sub> (eV)	LUCO <sub>calc</sub> (eV)	HOMO <sub>exp</sub> (eV)	LUMO <sub>exp</sub> (eV)	E <sub>g,calc</sub> (eV)
pSSS, P1	-3.96	-2.53	-3.93	-2.75	1.42
pSeSeSe, P2	-3.82	-2.66	-3.89	-2.79	1.15
pSeSse, P3	-3.9	-2.61	-3.81	-2.78	1.28
pSseS, P4	-3.96	-2.53	-3.97	-2.76	1.31
pSOS, P5	-4.13	-2.68	-4.03	-2.77	1.44
pSNC <sub>6</sub> S, P6	-3.76	-2.00	-4.1	-2.5	1.76
polymer A	-4.77	-3.14			1.63
polymer B	-4.59	-2.80			1.80

**Table 3.** Resistivity Studies of Various DAD Polymers and PEDOT

	doped <sup>a</sup> (Ω)	neutral (Ω)	max doping by air (Ω)	doping with BF <sub>3</sub> (Ω)
PEDOT	10 <sup>2</sup>	4 × 10 <sup>5</sup>	10 <sup>2</sup>	10 <sup>2</sup>
PSSS, P1	10 <sup>2</sup>	2 × 10 <sup>6</sup>	4 × 10 <sup>3</sup>	10 <sup>2</sup>
PSeSeSe, P2	10 <sup>2</sup>	2 × 10 <sup>6</sup>	2 × 10 <sup>4</sup>	10 <sup>2</sup>
PSOS, P5	10 <sup>2</sup>	2 × 10 <sup>6</sup>	3 × 10 <sup>3</sup>	10 <sup>2</sup>
pSN(C <sub>6</sub> )S, P6	10 <sup>2</sup>	1 × 10 <sup>6</sup>	3 × 10 <sup>3</sup> Ω	10 <sup>3</sup>

<sup>a</sup>The 10<sup>2</sup> Ω is a limit of instrument resistivity measurements.

caused a slight rise in NIR absorption reflecting only partial doping. When a stronger BPh<sub>3</sub> Lewis acid was applied, a more significant increase of polymer absorption in the NIR region

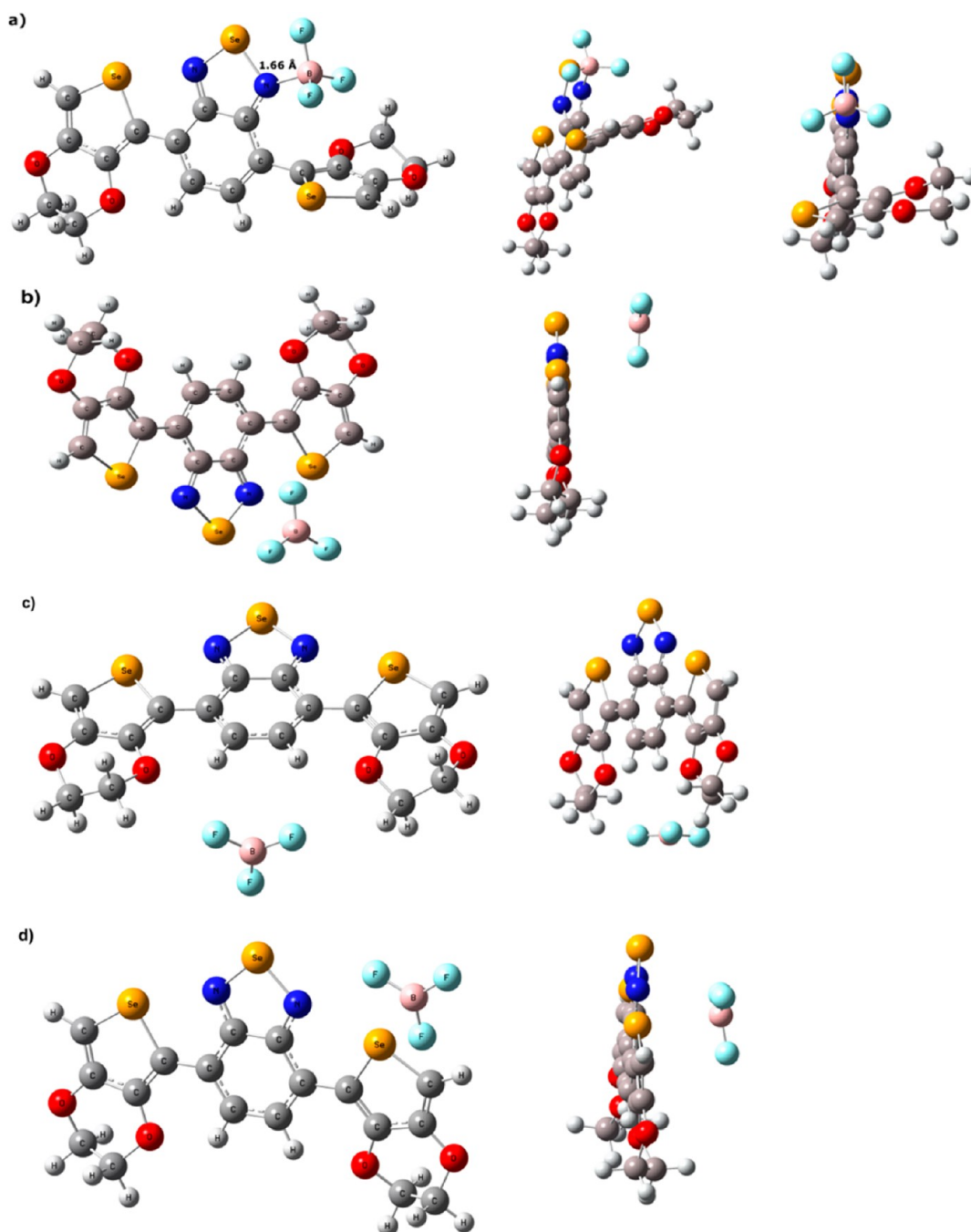


**Figure 6.** Different modes of Lewis acid ( $\text{BF}_3$ ) coordination to monomer 2. Left is front view, right is side view.

**Table 4. Calculated Energies for Different Modes of Lewis Acid ( $\text{BF}_3$ ) Coordination**

monomer	$\text{BF}_3$ location	$E_{\text{relative}}$ (kcal/mol)	HOMO (eV)	LUMO (eV)	$E_g$ (eV)
SeSeSe, 2 (a)	N-coordinated (a)	0	-5.39	-3.23	2.16
SeSeSe, 2 (b)	top (b)	8.2	-4.86	-2.59	2.26
SeSeSe, 2 (c)	side (c)	10.5	-4.81	-2.49	2.32
SeSeSe, 2 (d)	near Se (d)	3.8	-4.91	-2.54	2.38

was obtained revealing the more effective doping of all polymers. Finally, the reaction with the strong  $\text{BF}_3$  Lewis acid

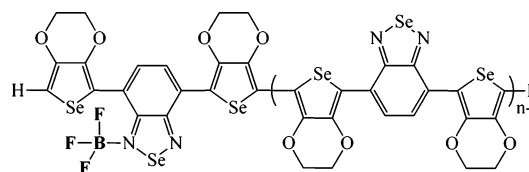


**Figure 7.** Oligomers  $(\text{SeSeSe})_n$ ,  $n = 3-6$ .

was performed, leading to high absorption intensity in the NIR region (close to that obtained by electrochemical doping). Thus, in all polymers strength of the applied Lewis acid correlates with the intensity of absorption spectra in near IR and consequently doping level of polymer giving the order  $\text{BF}_3 > \text{BPh}_3 > \text{BMe}_3$  (Figure 5).



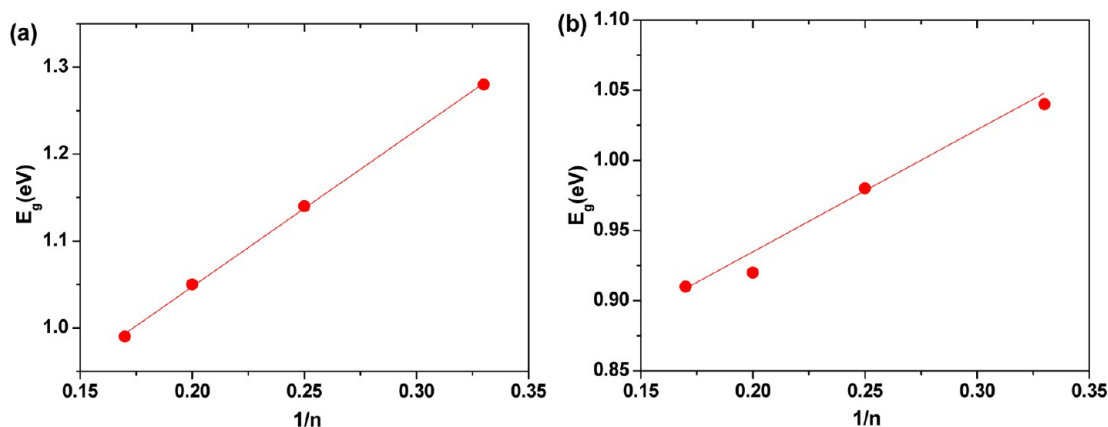
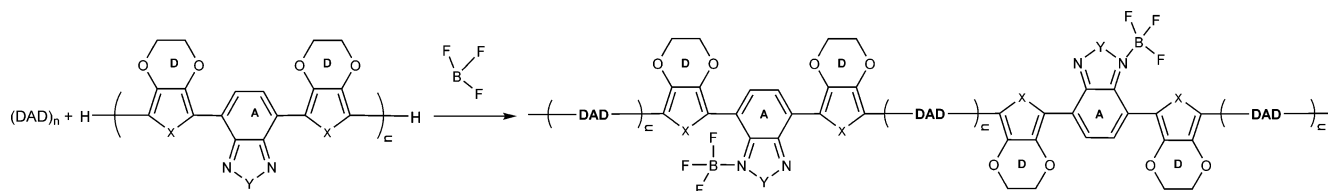


**Figure 8.** The HOMO–LUMO gap and linear fit of (a) oligomers (SeSeSe)<sub>n</sub> ( $n = 3–6$ ) with one coordinated Lewis acid (BF<sub>3</sub>) in each oligomer and (b) related polymers P(SeSeSe)<sub>n</sub> ( $n = 3–6$ ).

### Scheme 3. Proposed Mechanism and Doped Structure Formed by Reaction of DAD Polymers with Lewis Acid



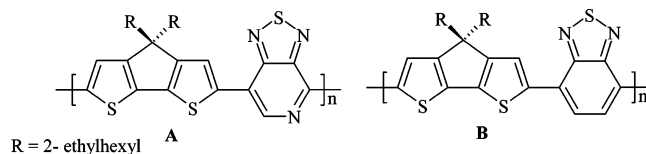
We have also found that doping and dedoping ability of polymers is strongly influenced by heteroatoms in their donor and acceptor moieties. It can be observed that treatment of pSSS, **P1** and pSSeS, **P4** polymers with BMe<sub>3</sub> causes only partial doping (Figure 5a,d), while pSeSeSe, **P2** and pSeSeSe, **P3** polymers that have Se atom in their donor fragments demonstrate relatively high doping levels even upon treatment with weak Lewis acid (Figure 5b,c). On the other hand, treatment of pSOS, **P5** and pSNC<sub>6</sub>S, **P6** polymers having O or N heteroatoms in the acceptor unit with BMe<sub>3</sub> did not cause any doping (Figure 5e,f). Thus, the soft Se atom in donor fragment increases doping ability of the resulting polymer, while presence of a hard heteroatom (O or N) in the acceptor unit significantly decreases the doping ability.

Regarding the dedoping ability, a hard heteroatom in the acceptor unit helps to achieve a good dedoping level even by applying a weak base. For instance, pSOS, **P5** polymer demonstrates nearly full conversion to the neutral state upon treatment with Et<sub>3</sub>N. On the other hand, incorporation of a soft Se atom into an acceptor unit decreases the dedopability of the polymer; thus, dedoping of pSeSeSe, **P2** and pSSeSe, **P4** with Et<sub>3</sub>N was poor.

**Correlation of HOMO Orbitals.** The experimental findings are also supported by orbital energy calculations. The polymers were fully optimized at the PBC/B3LYP/6-31G(d) level of theory (Table 2). It can be seen that polymers with Se atom in the donor fragment such as **P2** and **P3** have relatively high HOMO level energies. Consequently they can be easily doped upon treatment with even weak Lewis acids. On the other hand the polymers that have more stable HOMO energy levels, such as **P5** and **P6**, are capable to undergo chemical doping only with strong Lewis acids such as BF<sub>3</sub>.

To verify the importance of HOMO orbital energy we performed calculations of donor–acceptor structures reported by Bazan.<sup>24</sup> The polymers **A** and **B** are based on oligomers that were reported by Bazan to undergo remarkable band gap shift

upon coordination of Lewis acid; however, no doping was obtained. The polymers **A** and **B** were fully optimized at the PBC/B3LYP/6-31G(d) level of theory, and their orbital energies were calculated (Table 2).



The calculated results support the key role of HOMO energy levels stability for the ability of polymers to undergo nonoxidative doping. Polymers **A** and **B** have relatively stable HOCO  $-4.77$  and  $-4.59$  eV, respectively. Therefore they undergo band gap shift but not doping upon coordination of Lewis acid. The HOCO energies of polymers **P2–P5** reported in this work are significantly higher ( $-3.82$  to  $-4.13$  eV). This is because polymers **P2–P5** contain highly donating EDOS and EDOT moieties. EDOS and EDOT moieties cause increase of HOCO level energy and promote doping ability of the polymer. The difference between the HOCO energies of the polymers studied in this work clearly correlate with the ability of the corresponding polymers to undergo nonoxidative doping. **P2** has highest HOCO level energy ( $-3.82$  eV), and consequently it undergoes easiest doping by Lewis acid. On the other hand, **P5** has the most stable HOCO level energy ( $-4.13$  eV) in the series, and therefore its doping ability is lowest.

**Conductivity Changes.** The conductivity measurements of the represented polymers pSSS, **P1**; pSeSeSe, **P2**; pSOS, **P5**; and pSNC<sub>6</sub>S, **P6** were performed on interdigitated electrodes using a combination of chemical and electrochemical doping and dedoping methods (Table 3). It was found that DAD polymers are quite conductive in their doped state (85–110 Ω, which is actually the instrument measurement limit) and poorly conductive in their neutral state (1–2 MΩ). The DAD

polymers are relatively resistant to air doping, for instance, neutral **P2** remains undoped (20 k $\Omega$ ) even after prolonged exposure to air. This is in contrast to a non-donor–acceptor-type polymer, PEDOT, which undergoes fast doping by air and after 1 min reaches an almost fully doped state (300  $\Omega$ ). Thus, DAD polymers studied in this work are more stable toward air doping in their neutral state than PEDOT.

It was found that conductivity of the reported DAD polymers significantly changes upon treatment with Lewis acid that also reveals their doping. The conductivity studies correlate well with the UV–vis–IR results, where all DAD polymers, except **P6**, undergo effective chemical doping. Polymers **P1**, **P2**, and **P5** immediately became conductive when they were dipped in a CH<sub>2</sub>Cl<sub>2</sub> solution of BF<sub>3</sub>, while **P6** remained almost undoped and only after a prolonged time doping slowly begin to take place.

**Lewis Acid Coordination Geometry.** To elucidate the of mechanism of doping by Lewis acid, theoretical studies were performed using B3LYP/6-31G(d) level of theory. Different coordination positions of Lewis acid were considered to find the most favorable coordination mode of a dopant. A monomer unit of SeSeSe, **2** and BF<sub>3</sub> Lewis acid were used as model (Figure 6). It was found that the lowest energy is achieved when the BF<sub>3</sub> molecule is coordinated to the nitrogen atom and N–B length is 1.67 Å. The nitrogen atom is cramped inside two ethylenedioxy-selenophene units. Therefore, steric requirements enforce the ethylenedioxy-selenophene fragment to twist upon coordination of the BF<sub>3</sub> to nitrogen atom by 106° (Figure 6a). Other coordination modes result in energy increase by 3.8–10.5 kcal/mol (Figure 6b–d, Table 4 and Table S3, Supporting Information). The conformation with BF<sub>3</sub> coordinated to the nitrogen of acceptor fragment (conformation **a** in Figure 6) was used in polymer studies described below.

Twisting of the comonomer units by 106° caused by coordination of a Lewis acid is reflected in the decrease of conjugation level in the resulting polymer. The decrease in conjugation consequently increases the polymer band gap. When the polymer, bearing a BF<sub>3</sub> dopant in each monomer unit (polymer that consists of **2(a)**), was calculated, the band gap obtained was higher than that of the undoped state (1.38 vs 1.15 eV). This calculated result shows that an extensive doping by BF<sub>3</sub> leads to an extensive increase in the band gap of polymer and perhaps partial doping (with BF<sub>3</sub> present on only some monomer units) provides the more proper model.

Thus, a series of oligomers (SeSeSe)<sub>3</sub>, (SeSeSe)<sub>4</sub>, (SeSeSe)<sub>5</sub> and (SeSeSe)<sub>6</sub> consisting from 3, 4, 5, and 6 units of SeSeSe monomer, respectively, were studied (Table S4, Supporting Information). In each oligomer only one molecule of BF<sub>3</sub> was coordinated to the first SeSeSe unit as shown in Figure 7.

HOMO–LUMO gap values for (SeSeSe)<sub>n</sub> ( $n = 3–6$ ) are represented in Figure 8, where  $n$  is a number of monomer units of SeSeSe per one molecule of BF<sub>3</sub>. The more monomer units per one molecule of BF<sub>3</sub>, the lower band gaps are achieved. The maximum length of the oligomer that was calculated is 6 units of monomer SeSeSe, with one molecule of BF<sub>3</sub> that gives band gap of 0.99 eV (Figure 8a and Table S4, Supporting Information). Notably, when the second BF<sub>3</sub> molecule was added to this oligomer, the band gap increased to 1.08 eV (Table S4, Supporting Information). It can be seen in Figure 8a that an extrapolation to SeSeSe/ $n$ , where  $n$  is high number of monomer units of SeSeSe per one molecule of BF<sub>3</sub> (actually oligomer SeSeSe/ $n$  is a polymer of with one coordinated BF<sub>3</sub> molecule) gives a HOMO–LUMO gap of 0.69 eV (1770 nm).

To verify the presented model, polymers P(SeSeSe)<sub>n</sub> consisting of (SeSeSe)<sub>n</sub> ( $n = 3–6$ ), respectively, were calculated. Very similar results were observed, and extrapolation to  $1/n \rightarrow 0$  gave a band gap of 0.76 eV (Figure 8b). Thus, the best band gap decrease is reached upon partial doping by Lewis acid (one BF<sub>3</sub> molecule per many units of DAD).

The computational results correlate with our experimental observations. Addition of excessive amount of Lewis acid does not decrease the band gap in UV–vis–IR spectra. Our computational findings also correlate with previous works, where steric hindrance and planarity concerns dictate the boron moiety coordination mode. For instance, Bazan observed a distortion from planarity by nearly 60° upon borane coordination to the azole N-atoms.<sup>24</sup> On the other hand, borane coordination to the N-atom results in only 25° distortion from planarity that provides one of the important reasons for the borane coordination preference.<sup>24</sup> Distortion in our case is ~106° (for oligomers) and in average 102° (for polymers).

Thus, we propose the following mechanism of chemical doping of DAD polymers **P1–P6**: (1) Doping takes place upon coordination of Lewis acid to a nitrogen atom of acceptor unit. (2) Upon coordination, acid twisting of the polymer backbone occurs. (3) To reduce the negative effect on conjugation upon twisting, Lewis acid molecules coordinate not to every comonomer unit but one per several monomers. This is sufficient for doping but does not cause dramatic conjugation loss (Scheme 3).

## CONCLUSIONS

In this work we reported unprecedented nonoxidative doping of donor–acceptor–donor polymers. We designed a series of new polymers that can undergo switching from neutral to doped state upon Lewis acid coordination, while decoordination of Lewis acid by external base caused the return from doped to neutral state. The reported doping and dedoping approach results in notable polymer conductivity changes and optical switching. The polymers show remarkable stability after numerous switching cycles and can be switched both electrochemically and chemically. The ability of the corresponding polymers to undergo nonoxidative doping or dedoping clearly correlates with their HOCO energy. The structure of the doped polymers was modeled by computational studies suggesting partial coordination of Lewis acid (one BF<sub>3</sub> molecule for multiple units of monomer). Such a coordination mode is sufficient to obtain doping, but does not affect conjugation and allows for an effective band gap decrease.

In conclusion, the reported nonoxidative doping approach is a reversible, nondestructive and can be precisely regulated by the strength of the applied chemical reagent. This doping type does not involve electron transfer and opens up the new possibility to control conjugation, color and conductivity of conjugated polymers.

## ASSOCIATED CONTENT

### Supporting Information

Additional electrochemical and spectroelectrochemical data, crystal data (CIF), optimized geometries for the ground state (B3LYP/6-31G(d)) and Cartesian coordinates, and calculated HOCO and LUCO energies. This material is available free of charge via the Internet at <http://pubs.acs.org>.

## ■ AUTHOR INFORMATION

## Corresponding Author

elenap@volcani.agri.gov.il

## Present Addresses

<sup>‡</sup>Department of Food Quality and Safety, Agricultural Research Organization, The Volcani Center, Bet Dagan, 50250, Israel.<sup>†</sup>Physics of Energy Harvesting Division, CSIR-National Physical Laboratory, New Delhi-110012, India.

## Notes

The authors declare no competing financial interest.

## ■ ACKNOWLEDGMENTS

We thank the Israel Science Foundation (ISF) and the Helen and Martin Kimmel Center for Molecular Design for financial support.

## ■ DEDICATION

<sup>†</sup>In memory of Professor Michael Bendikov.

## ■ REFERENCES

- (1) (a) *Handbook of Conducting Polymers*, 3rd ed.; Skotheim, T. A., Reynolds, J. R., Eds.; CRC Press: Boca Raton, FL, 2007. (b) *Handbook of Organic Conductive Molecules and Polymers*; Nalwa, H. S., Ed.; J. Wiley & Sons: New York, 1997.
- (2) MacDiarmid, A. G. *Angew. Chem., Int. Ed.* **2001**, *40*, 2581–2590.
- (3) (a) Facchetti, A. *Mater. Today* **2007**, *10*, 28–37. (b) *Organic Field-Effect Transistors*; Bao, Z., Locklin, J., Eds.; CRC Press: New York, 2007.
- (4) (a) *Handbook of Thiophene-Based Materials*; Perepichka, I. F., Perepichka, D. F., Eds.; Wiley-VCH: Chichester, U.K., 2009. (b) Perepichka, I. F.; Perepichka, D. F.; Meng, H.; Wudl, F. *Adv. Mater.* **2005**, *17*, 2281–2305.
- (5) (a) Marsella, M. J.; Reid, R. J.; Estassi, S.; Wang, L. S. *J. Am. Chem. Soc.* **2002**, *124*, 12507–12510. (b) Jager, E. W. H.; Smela, E.; Inganäs, O. *Science* **2000**, *290*, 1540–1546.
- (6) McQuade, D. T.; Pullen, A. E.; Swager, T. M. *Chem. Rev.* **2000**, *100*, 2537–2574.
- (7) (a) Yu, G.; Gao, J.; Hummelen, J. C.; Wudl, F.; Heeger, A. J. *Science* **1995**, *270*, 1789–1791. (b) Sariciftci, N. S.; Smilowitz, L.; Heeger, A. J.; Wudl, F. *Science* **1992**, *258*, 1474–1476. (c) Liang, Y.; Feng, D.; Wu, Y.; Tsai, S.-T.; Li, G.; Ray, C.; Yu, L. *J. Am. Chem. Soc.* **2009**, *131*, 7792–7799. (d) Park, S. H.; Roy, A.; Beaupre, S.; Cho, S.; Coates, N.; Moon, J. S.; Moses, D.; Leclerc, M.; Lee, K.; Heeger, A. J. *Nat. Photonics* **2009**, *3*, 297–303.
- (8) Barnes, W. L.; Samuel, I. D. W. *Science* **1999**, *285*, 211–212.
- (9) (a) Bhadra, S.; Khastgir, D.; Singha, N. K.; Lee, J. H. *Prog. Polym. Sci.* **2009**, *34*, 783–810. (b) Varela-Alvarez, A.; Sordo, J. A.; Scuseria, G. E. *J. Am. Chem. Soc.* **2005**, *127*, 11318–11327. (c) Chaudhuri, D.; Kumar, A.; Rudra, I.; Sarma, D. D. *Adv. Mater.* **2001**, *13*, 1548–1551.
- (10) (a) Bienkowski, K.; Kulszewicz-Bajer, I.; Genoud, F.; Oddou, J. L.; Pron, A. *Synth. Met.* **2003**, *135*–136. (b) Kulszewicz-Bajer, I.; Pron, A.; Abramowicz, J.; Jeandey, C.; Oddou, J.-L.; Sobczak, J. W. *Chem. Mater.* **1999**, *11*, 552–556. (c) Genoud, F.; Kulszewicz-Bajer, I.; Dufour, B.; Rannou, P.; Pron, A. *Synth. Met.* **2001**, *119*, 415–416.
- (11) (a) Wang, H.; Helgeson, R.; Ma, B.; Wudl, F. *J. Org. Chem.* **2000**, *65*, 5862–5867. (b) Irvin, D. J.; DuBois, C. J., Jr.; Reynolds, J. R. *Chem. Comm.* **1999**, 2121–2122. (c) Berets, D. J.; Smith, D. S. *Trans. Faraday Soc.* **1968**, *64*, 823–8. (d) Kaul, S. N.; Fernandez, J. E. *Macromolecules* **1987**, *20*, 2320–2.
- (12) It was found that the polymerization of conductive polymers in the presence of Lewis acid leads to a significant improvement in polymer film quality. For examples, see: (a) Can, M.; Oezaslan, H.; Isildak, O.; Pekmez, N. O.; Yildiz, A. *Polymer* **2004**, *45*, 7011–7016. (b) Alkan, S.; Cutler, C. A.; Reynolds, J. R. *Adv. Funct. Mater.* **2003**, *13*, 331–336. (c) Baik, W.; Luan, W.; Zhao, Ren H.; Koo, S.; Kim, K.-S. *Synth. Met.* **2009**, *159*, 1244–1246. (d) Chen, W.; Xue, G. *Prog. Polym. Sci.* **2005**, *30*, 783–811. (e) Focante, F.; Mercandelli, P.; Sironi, A.; Resconi, L. *Coord. Chem. Rev.* **2006**, *250*, 170.
- (13) (a) Monk, P. M. S.; Mortimer, R. J.; Rosseinsky, D. R. In *Electrochromism and Electrochromic Devices*; Cambridge University Press: New York, 2007; Chapter 4. (b) Guzman, A. R.; Harpham, M. R.; Suzer, O.; Haley, M. M.; Goodson, T. G. *J. Am. Chem. Soc.* **2010**, *132*, 7840–7841.
- (14) (a) Heeney, M.; Zhang, W.; Crouch, D. J.; Chabynyc, M. L.; Gordeyev, S.; Hamilton, R.; Higgins, S. J.; McCulloch, I.; Skabara, P. J.; Sparrowe, D.; Tierney, S. *Chem. Commun.* **2007**, 5061–5063. (b) Sonmez, G.; Meng, H.; Wudl, F. *Chem. Mater.* **2003**, *15*, 4923–4929. and references therein. (c) Lee, B.; Yavuz, M. S.; Sotzing, G. A. *Macromolecules* **2006**, *39*, 3118–3124. (d) Lee, B.; Seshadri, V.; Palko, H.; Sotzing, G. A. *Adv. Mater.* **2005**, *17*, 1792–1795.
- (15) (a) Mozer, A. J.; Sariciftci, N. S. In *Handbook of Conducting Polymers: Processing and Applications*, 3rd ed.; Skotheim, T. A., Reynolds, J. R., Eds.; CRC Press: Boca Raton, FL, 2007; Chapter 10, pp 10.1–10.37. (b) Facchetti, A. *Chem. Mater.* **2011**, *23*, 733–758. (c) Mishra, A.; Ma, C. Q.; Bäuerle, P. *Chem. Rev.* **2009**, *109*, 1141–1276. (d) Cheng, Y. J.; Yang, S. H.; Hsu, C. S. *Chem. Rev.* **2009**, *109*, 5868. (e) Cai, W. Z.; Gong, X.; Cao, Y. *Sol. Energy Mater. Sol. Cells* **2010**, *94*, 114–127. (f) Nelson, J. *Mater. Today* **2011**, *14*, 462–470. (g) Brabec, C. J.; Gowrisanker, S.; Halls, J. J. M.; Laird, D.; Jia, S.; Williams, S. P. *Adv. Mater.* **2010**, *22*, 3839–3856.
- (16) (a) Facchetti, A. *Mater. Today* **2013**, *16*, 123. (b) Chen, H.-Y.; Hou, J.; Zhang, S.; Liang, Y.; Yang, G.; Yang, Y.; Yu, L.; Wu, Y.; Li, G. *Nat. Photonics* **2009**, *3*, 649–653 and references therein. (c) Sariciftci, N. S.; Smilowitz, L.; Heeger, A. J.; Wudl, F. *Science* **1992**, *258*, 1474–1476. (d) Liang, Y.; Feng, D.; Wu, Y.; Tsai, S.-T.; Li, G.; Ray, C.; Yu, L. *J. Am. Chem. Soc.* **2009**, *131*, 7792–7799. (e) Park, S. H.; Roy, A.; Beaupre, S.; Cho, S.; Coates, N.; Moon, J. S.; Moses, D.; Leclerc, M.; Lee, K.; Heeger, A. J. *Nat. Photonics* **2009**, *3*, 297–303. (f) Huo, L.; Hou, J.; Zhang, S.; Chen, H.-U.; Yang, Y. *Angew. Chem., Int. Ed. Engl.* **2009**, *49*, 1500–1503. (g) Wang, M.; Hu, X.; Liu, P.; Li, W.; Gong, X.; Huang, F.; Cao, Y. *J. Am. Chem. Soc.* **2011**, *133*, 9638–9641.
- (17) (a) Perepichka, D. F.; Perepichka, I. F.; Meng, H.; Wudl, F. In *Organic Light-Emitting Materials and Devices*; Li, Z., Meng, H., Eds.; CRC Press: Boca Raton, FL, 2007; Chapter 2, pp 45–293. (b) Groenendaal, L.; Zotti, G.; Aubert, P.-H.; Waybright, S. M.; Reynolds, J. R. *Adv. Mater.* **2003**, *15*, 855–879. (c) Mortimer, R. J.; Dyer, A. L.; Reynolds, J. R. *Displays* **2006**, *27*, 2–18. (d) Balan, A.; Baran, D.; Toppare, L. *Polym. Chem.* **2011**, *2*, 1029–1043. (e) Jiang, H.; Taranekekar, P.; Reynolds, J. R.; Schanze, K. S. *Angew. Chem., Int. Ed.* **2009**, *48*, 4300–4316.
- (18) (a) Beaujuge, P. M.; Ellinger, S.; Reynolds, J. R. *Nat. Mater.* **2008**, *7*, 795–799. (b) Xia, Y.; Wang, L.; Deng, X.; Li, D.; Zhu, X.; Cao, Y. *Appl. Phys. Lett.* **2006**, *89*, 081106. (c) Steckler, T. T.; Abboud, K. A.; Craps, M.; Rinzler, A. G.; Reynolds, J. R. *Chem. Commun.* **2007**, 4904–4906. (d) Sonmez, G.; Meng, H.; Wudl, F. *Chem. Mater.* **2003**, *15*, 4923–4929. (e) Zhu, Y.; Champion, R. D.; Jenekhe, S. A. *Macromolecules* **2006**, *39*, 8712–8719. (f) Salzner, U. *J. Phys. Chem. B* **2002**, *106*, 9214–9220. (g) Ajayaghosh, A. *Chem. Soc. Rev.* **2003**, *32*, 181–191.
- (19) (a) Hou, J.; Chen, H. Y.; Zhang, S.; Li, G.; Yang, Y. *J. Am. Chem. Soc.* **2008**, *130*, 16144. (b) Peet, J.; Kim, Y.; Coates, N. E.; Ma, W. L.; Moses, D.; Heeger, A. J.; Bazan, G. C. *Nat. Mater.* **2007**, *6*, 497. (c) Kim, J. Y.; Lee, K.; Coates, N. E.; Moses, D.; Nguyen, T. Q.; Dante, M.; Heeger, A. J. *Science* **2007**, *317*, 222. (d) Thomas, C. A.; Zong, K.; Abboud, K. A.; Steel, P. J.; Reynolds, J. R. *J. Am. Chem. Soc.* **2004**, *126*, 16440–16450. (e) Chevallier, F.; Charlot, M.; Katan, C.; Mongin, F.; Blanchard-Desce, M. *Chem. Commun.* **2009**, *6*, 692–694.
- (20) (a) Akoudad, S.; Roncali, J. *Synth. Met.* **1999**, *101*, 149. (b) Groenendaal, L. B.; Jonas, F.; Freitag, D.; Pielartzik, H.; Reynolds, J. R. *Adv. Mater.* **2000**, *12*, 481–494. (c) Groenendaal, L. B.; Zotti, G.; Aubert, P.-H.; Waybright, S. M.; Reynolds, J. R. *Adv. Mater.* **2003**, *15*, 855–879. (d) Zhang, X.; Steckler, T. T.; Dasari, R. R.; Ohira, S.; Potscavage, W. J.; Tiwari, S. P.; Coppee, S.; Ellinger, S.; Barlow, S.; Bredas, J. L.; Kippelen, B.; Reynolds, J. R.; Marder, S. R. *J. Mater. Chem.* **2010**, *20*, 123–134.

(21) (a) Xu, S.; Liu, Y.; Li, J.; Wang, Y.; Cao, S. *Polym. Adv. Technol.* **2010**, *21*, 663–668. (b) Kim, J.; Park, S. H.; Cho, S.; Jin, Y.; Kim, J.; Kim, I.; Lee, J. S.; Kim, J. H.; Woo, H. Y.; Lee, K.; Suh, H. *Polymer* **2010**, *51*, 390–396. (c) Sun, X.; Xu, X.; Qiu, W.; Yu, G.; Zhang, H.; Gao, X.; Chen, S.; Song, Y.; Liu, Y. *J. Mater. Chem.* **2008**, *18*, 2709–2715. (d) Morikita, T.; Yamaguchi, I.; Yamamoto, T. *Adv. Mater.* **2001**, *13*, 1862–1864.

(22) Welch, G. C.; Coffin, R.; Peet, J.; Bazan, G. C. *J. Am. Chem. Soc.* **2009**, *131*, 10802–10803.

(23) Welch, G. C.; Bazan, G. C. *J. Am. Chem. Soc.* **2011**, *133*, 4632–4644.

(24) (a) Zalar, P.; Henson, Z. B.; Welch, G. C.; Bazan, G. C.; Nguyen, T.-Q. *Angew. Chem., Int. Ed.* **2012**, *51*, 7495–7498. (b) Zalar, P.; Kuik, M.; Henson, Z. B.; Woellner, C.; Zhang, Y.; Sharenko, A.; Bazan, G. C.; Nguyen, T.-Q. *Adv. Mater.* **2013**, *25*, 1.

(25) Durmus, A.; Gunbas, G. E.; Camurlu, P.; Toppare, L. *Chem. Commun.* **2007**, *31*, 3246–3248.

(26) Cihaner, A.; Algi. *Adv. Funct. Mater.* **2008**, *18*, 3583–3589.

(27) Zhu, S. S.; Swager, T. M. *J. Am. Chem. Soc.* **1997**, *119*, 12568–12577.

(28) (a) Tsubata, Y.; Suzuki, T.; Miyashi, T.; Yamashita, Y. *J. Org. Chem.* **1992**, *57*, 6749. (b) Yang, R.; Tian, R.; Yan, J.; Zhang, Y.; Jian Yang, Y.; Hou, Q.; Yang, W.; Zhang, C.; Cao, Y. *Macromolecules* **2005**, *38*, 244–253.

(29) Blouin, N.; Michaud, A.; Gendron, D.; Wakim, S.; Blair, E.; Neagu-Plesu, R.; Belletete, M.; Durocher, G.; Tao, Y.; Leclerc, M. *J. Am. Chem. Soc.* **2008**, *130*, 732–742.

(30) Tanimoto, A.; Yamamoto, T. *Adv. Synth. Catal.* **2004**, *346*, 1818–1823.

(31) Yalcinkaya, F.; Powner, E. T. *Med. Eng. Phys.* **1997**, *19*, 299–301.

(32) Connelly, N. G.; Geiger, W. E. *Chem. Rev.* **1996**, *96*, 877.

(33) Kulkarni, A.; Tonzola, C.; Babel, A.; Jenekhe, S. *Chem. Mater.* **2004**, *16*, 4556–4573.

(34) We note that different values in the range of 4.4–4.8 eV are used to transform the energy level of SCE to the energy of the HOMO. See: (a) D'Andrade, B. W.; Datta, S.; Forrest, S. R.; Djurovich, P.; Polikarpov, E.; Thompson, M. E. *Org. Electron.* **2005**, *6*, 11. (b) Djurovich, P. I.; Mayo, E. I.; Forrest, S. R.; Thompson, M. E. *Org. Electron.* **2009**, *10*, 515. (c) Cardona, C. M.; Li, W.; Kaifer, A. E.; Stockdale, D.; Bazan, G. C. *Adv. Mater.* **2011**, *23*, 2367.

(35) Frisch, M. J., et al. *Gaussian 09*, Revision A.02; Gaussian, Inc.: Wallingford, CT, 2009.

(36) (a) Parr, R. G.; Yang, W. *Density-Functional Theory of Atoms and Molecules*; Oxford University Press: New York, 1989. (b) Koch, W.; Holthausen, M. C. *Chemist's Guide to Density Functional Theory*; Wiley-VCH: New York, 2000. (c) Lee, C.; Yang, W.; Parr, R. G. *Phys. Rev. B: Condens. Matter Mater. Phys.* **1988**, *37*, 785. (d) Becke, A. D. *J. Chem. Phys.* **1993**, *98*, 5648.

(37) Patra, A.; Wijsboom, Y. H.; Zade, S. S.; Li, M.; Sheynin, Y.; Leitius, G.; Bendikov, M. *J. Am. Chem. Soc.* **2008**, *130*, 6734–6736.

(38) Wong, W.-Y.; Wang, X.; Zhang, H.-L.; Cheung, K.-Y.; Fung, M.-K.; Djuricic, A. B.; Chan, W.-K. *J. Organomet. Chem.* **2008**, *693*, 3603.

(39) Steckler, T. T.; Abboud, K. A.; Craps, M.; Rinzler, A. G.; Reynolds, J. R. *Chem. Commun.* **2007**, 4904.

(40) The CV of P1 polymer was reported previously in ref 25.

(41) (a) Patra, A.; Bendikov, M. *J. Mater. Chem.* **2010**, *20*, 422–433. (b) Wijsboom, Y. H.; Patra, A.; Zade, S. S.; Sheynin, Y.; Li, M.; Shimon, L. J. W.; Bendikov, M. *Angew. Chem., Int. Ed.* **2009**, *48*, 5443–5447. (c) Wijsboom, Y. H.; Sheynin, Y.; Patra, A.; Zamoshchik, N.; Vardimon, R.; Leitius, G.; Bendikov, M. *J. Mater. Chem.* **2011**, *21*, 1368.

(42) Li, M.; Sheynin, Y.; Patra, A.; Bendikov, M. *Chem. Mater.* **2009**, *21*, 2482–2488.

(43) To reveal the importance of Lewis acid coordination, reaction of the presented polymers with HCl was performed. No doping was obtained. To exclude a possibility of oxidative electron transfer, reaction of PEDOT polymer with Lewis acid was performed. No doping was obtained. For more details, see the Supporting Information.